

Spontaneous fission properties of ^{258}Fm , ^{259}Md , ^{260}Md , ^{258}No , and $^{260}\text{[104]}$: Bimodal fission

E. K. Hulet, J. F. Wild, R. J. Dougan, R. W. Lougheed, J. H. Landrum, A. D. Dougan,
P. A. Baisden, C. M. Henderson, and R. J. Dupzyk
University of California, Lawrence Livermore National Laboratory, Livermore, California 94551

R. L. Hahn*

Oak Ridge National Laboratory, Oak Ridge, Tennessee 37830

M. Schädel and K. Sümmerer

Gesellschaft für Schwerionenforschung, 6100 Darmstadt, Federal Republic of Germany

G. R. Bethune[†]

Bethune-Cookman College, Daytona Beach, Florida 32015

(Received 28 December 1988)

We have measured the mass and kinetic-energy distributions from the spontaneous fission of ^{258}Fm , ^{258}No , ^{259}Md , ^{260}Md , and $^{260}\text{[104]}$. All are observed to fission with a symmetrical division of mass. The total-kinetic-energy distributions strongly deviated from the Gaussian shape characteristically found in the fission of all other actinides. When the total-kinetic-energy distributions are resolved into two Gaussians, the constituent peaks lie near 200 and 233 MeV. We conclude that both low- and high-energy fission modes occur in four of the five nuclides studied. We call this property "bimodal fission." Even though both modes are possible in the same nuclide, one generally predominates. We offer an explanation for each mode based on shell structures of the fissioning nucleus and of its fragments. The appearance of both modes of fission in this region of the nuclide chart seems to be a coincidence in that the opportunity to divide into near doubly magic Sn fragments occurs in the same region where the second fission barrier is expected to drop in energy below the ground state of the fissioning nucleus. Appropriate paths on the potential-energy surface of deformation have been found by theorists, but no physical grounds have been advanced that would allow the near equal populations we observe traveling each path. We suggest that this failure to find a reason for somewhat equal branching may be a fundamental flaw of current fission models. Assuming the proposed origins of these modes are correct, we conclude the low-energy, but also mass-symmetrical mode is likely to extend to far heavier nuclei. The high-energy mode will be restricted to a smaller region, a realm of nuclei defined by the proximity of the fragments to the strong neutron and proton shells in ^{132}Sn . We present some concluding remarks on the present state of fission theory and indicate a potential redirection that might be taken.

I. INTRODUCTION

In an earlier Letter,¹ we presented evidence that four of the five nuclides listed in the title undergo two distinguishable modes of spontaneous fission. One mode is characterized by broad, symmetrical mass distributions and fragment energies in accord with liquid-drop expectations, whereas the other mode produces sharply symmetrical mass distributions with total kinetic energies (TKE) of the fragments approaching the Q values for the fission reaction. Both modes are possible in the same nuclide, but one generally predominates. These modes lead to distinctly different TKE distributions, the observed TKE distribution being the sum of the contributions of both modes. Thus, we found TKE distributions that deviated strongly from the Gaussian shapes normally found in the fission of lighter actinides.

The purpose of this paper is to provide details of the

experiments, the fission properties of the five nuclides, and additional conclusions that can be derived from the results. Our motivation for investigating the spontaneous fission (SF) properties of these very heavy nuclides was to further explore a particularly interesting region beyond the heavy fermium isotopes, where we and others had found a sudden onset of mass symmetry and high fragment energies in neutron-induced fission and spontaneous fission. Elsewhere on the nuclide chart, only the isotopes of the elements Hg through Ac fission with symmetrical mass distributions at low-excitation energies.² Asymmetrical (two-humped) mass distributions are a common feature in low-energy-induced and spontaneous fission of the actinides until ^{258}Fm is reached. The very sharply symmetrical mass distributions and average TKE's near 240 MeV found for ^{258}Fm (Refs. 3 and 4) and ^{259}Fm (Ref. 5) are remarkable. To determine the range of this behavior, to provide critical tests of theory, and to improve our

predictions for heavier and more distant nuclei, it was necessary to extend these fission studies to nuclides with greater atomic and neutron numbers.

An opportunity to study the balance of forces between the macroscopic and microscopic components that make up the fission barrier was another factor that prompted our investigation. A major portion of the fission barrier for lighter nuclei is imparted by the liquid-drop (macroscopic) component, but its contribution diminishes rapidly with increasing Z because of the squared expansion of the Coulomb repulsive force. However, the total height of the fission barrier is the sum of the macroscopic portion and a microscopic part produced by shell effects from spin-orbit interactions, pairing, etc. Upon reaching element 100 (Fm), the contribution to the barrier by the macroscopic part drops to less than a third of the total, the remainder being due to shell stabilization of the deformed ground states. Nuclei with $Z \geq 106$, particularly the predicted superheavy elements, owe their entire stability against SF to barriers derived from shell effects.⁶ Hence, the nuclei we proposed to study between $Z = 100$ and 104 were directly in the region where the effects on fission properties induced by liquid-drop potential energies should largely fade and be replaced by those from shell energies. Knowing the enormous impact of fragment shells on the SF properties of ^{258}Fm and ^{259}Fm , we might now hope to assess the changes in fission wrought by the intrinsic structure of the fissioning nucleus.

All of the nuclides we have studied were selected on the basis of having neutron numbers ≥ 156 and atomic numbers ≥ 100 . In addition to the reasons given above, this region was chosen because both experimental SF half-lives and theory⁷⁻⁹ indicated the outer peak of the "double-humped" fission barrier was dropping in energy below the ground state for such nuclides. This was believed to be one factor in the sharp departure from the fission behavior of the lighter actinides. Moreover, the principal cause being advanced for the unusual fission properties of ^{258}Fm and ^{259}Fm was strong shell effects in the emerging fission-product nuclei, which were driving the reaction toward the doubly magic ^{132}Sn nucleus.¹⁰⁻¹² Thus, the transition from asymmetrical mass division in the light fermium isotopes to symmetrical in the heavier ones, would be due to fragments approaching closed proton and neutron shells ($Z = 50$, $N = 82$).¹³ By studying heavier nuclei, we could establish the range of Z and N where fission properties were being influenced by closed-shell fragments. This would be a further test of the predictions of the two-center shell model, because this model predicted a return to an asymmetrical division of mass when Z was increased beyond 100, while maintaining N essentially constant.⁹

Because it is exceedingly difficult to produce more than 300 or 400 atoms of these isotopes, our measurements of their fission properties have been restricted to determining the energies of coincident fragments. The sum of these energies provides the TKE, while the masses of the fragments are deduced from an inverse relationship between mass and fragment energies due to the conservation of momentum and an assumption that mass is conserved. Since neutrons are emitted from the fragments in

flight, we can only record the postneutron kinetic energies of the fragments. Neither these energies nor the derived masses have been corrected for the kinematics of neutron emission because neutron-multiplicity measurements as a function of mass or energy division are unavailable (and probably unattainable except for ^{260}Md).¹⁴ In principle, we could attempt to correct our provisional mass and TKE distributions by extrapolating the neutron multiplicities obtained for ^{252}Cf or ^{257}Fm . However, because the fission properties of these two nuclides are so radically different from the ones reported here, any extrapolation would be no better than a guess.

In Sec. II, we describe the production methods and fission measurements for each isotope in turn. Sec. III provides the results, and the last Sec. IV includes a comprehensive discussion of these results, their implications, and the significant conclusions drawn.

II. EXPERIMENT

A. 21-ms $^{260}\text{[104]}$

Controversy has surrounded this nuclide since 1964 when the Joint Institute for Nuclear Research (JINR) at Dubna assigned a 300-ms SF activity to this isotope of element 104.¹⁵ Later experiments by the JINR group^{16,17} reduced the half-life to 80 ms, but this decay period was never found by a group from the National Laboratories in the United States.¹⁸ Instead, a 23 ± 2 -ms SF decay period was found in bombardments of ^{249}Bk with ^{15}N . Eventually, these divergences in determining the half-life were resolved by further experiments at the JINR, where they obtained a 28 ± 6 -ms period,¹⁹ and at the Lawrence Berkeley Laboratory, where Somerville reported 21 ± 1 ms.²⁰ We obtained a rough half-life of 26 ± 7 ms in this work (Fig. 1), which is consistent with these most recent measurements.²¹

This short-lived SF isotope has been produced in the reactions $^{249}\text{Bk}(^{15}\text{N}, 4n)$, $^{248}\text{Cm}(^{16}\text{O}, 4n)$, and $^{249}\text{Cf}(^{18}\text{O}, \alpha 3n)$ with cross section of 14, 6, and 9 nb, re-

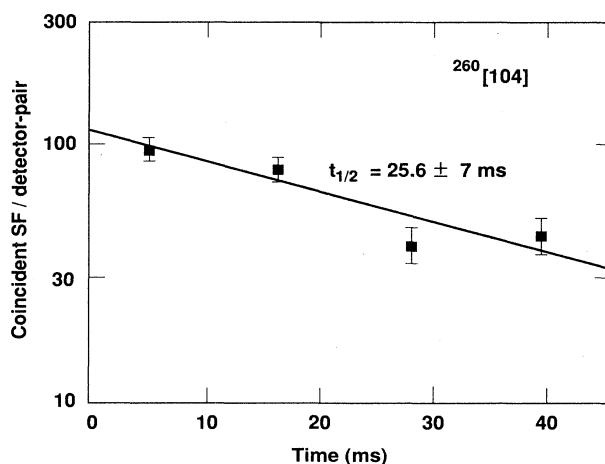


FIG. 1. Spontaneous-fission half-life of $^{260}\text{[104]}$ obtained in the SWAMI instrument from fission counts per detector station vs rotation time.

spectively.²⁰ We chose the $^{249}\text{Bk} + ^{15}\text{N}$ reaction because of the higher formation cross section for $^{260}\text{[104]}$. The energy of the projectile entering the target from the 88-in. cyclotron at the Lawrence Berkeley Laboratory was 81.6 MeV, which is at the peak of the excitation function. We averaged 4×10^{12} particles/s, an intensity that was about half of the destruction limit set by overheating of the targets. Two targets were made, consisting of 0.22 and 0.30 mg cm^{-2} of ^{249}Bk sublimed as the trifluoride within a 6-mm-diam circle onto 2.51 mg cm^{-2} Be foils.²² We mounted these and all target foils in a modular target system that provides maximum cooling by jetting 0.7 l s^{-1} of N_2 against the rear surface of the target backing foil.²³

A new instrument, SWAMI (spinning-wheel analyzer for millisecond isotopes), was designed and constructed for the purpose of obtaining the fission properties of very short-lived SF isotopes. Although it will be described more fully elsewhere,²⁴ a schematic diagram showing the principle of its operation is given in Fig. 2. Products of the nuclear reactions are ejected from the target by recoil momentum and are partially stopped in a continuous band of thin aluminum foils mounted on the outer edge of a rotating disk. These foils then pass between four pairs of trapezoidally shaped, surface-barrier detectors that measure the energies of the coincident fission fragments when the recoil product decays by SF. The disk, with a diameter of 30 cm, can be rotated at preset speeds

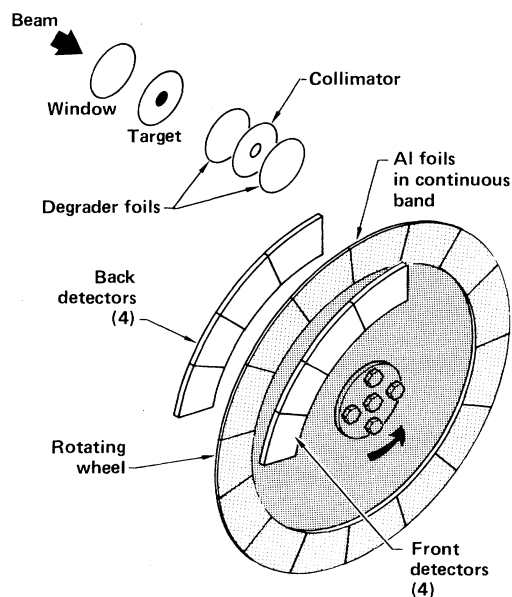


FIG. 2. Schematic diagram showing the essential features of the SWAMI instrument. A portion of the recoil products emerging from the target is stopped in $100\text{-}\mu\text{g cm}^{-2}$ Al foils that are located in a band surrounding the continuously rotating disk. These foils rotate between four pairs of surface-barrier detectors that measure the energy deposited by correlated fission fragments when the product nuclei decay by spontaneous fission.

between 10 and 5000 rpm (revolutions per minute). We used 260 rpm in these experiments in order to optimize the fraction of the 21-ms activity decaying within the detector segment.

The SWAMI instrument is especially suited for the study of millisecond SF nuclides originating from compound-nucleus reactions where the recoil energies of the products are below 5 MeV and nearly monoenergetic. The instrument was designed to discriminate against products from transfer reactions on the basis of both recoil energy and angular distribution. Placement of a collimator and energy-degrader foils at the exit side of the target allowed only nuclei recoiling within a 17° angle from the beam axis to reach the $100\text{-}\mu\text{g cm}^{-2}$ Al collector foils, located on the outer rim of the rotating disk. The degrader foils of $114\text{-}\mu\text{g cm}^{-2}$ Al served to reduce the range of the desired recoil product in the collector foils to the point where about half were calculated to be stopped. Because products from transfer reactions have broad angular distributions and recoil energies exceeding those from compound-nucleus reactions, we were able to reduce the SF contribution from such products ($^{256}\text{Md}/^{256}\text{Fm}$) by about a factor of 6 over what it would have been otherwise.

Cross sections for the formation of various nuclides produced by transfer reactions were determined in separate experiments. An Al foil with the same areal density as the SWAMI collector foils, followed by two Au foils, each of 2.28 mg cm^{-2} , were placed behind the ^{249}Bk target to stop and collect all recoil products emerging from the target within a 31° cone. Irradiations of 66 min and 422 min were made on separate sets of foils; the Au foils were then dissolved and the elements Es through Md chemically separated. In the Au foils, yields for the Es isotopes with masses 249–256, the Fm isotopes with $A = 250\text{--}256$, and ^{256}Md were measured by analysis of α -particle energies, SF decay, and half-lives. The Al collector foils were not chemically processed, but the yields of a number of isotopes of Es and Fm, and of ^{256}Md , were determined by direct alpha and fission counting. The peak yield in the Es isotopes occurred between $A = 251$ and 252 with a $176\text{-}\mu\text{b}$ cross section for the fraction stopped in the Au foils. The Fm yields peaked at the same mass numbers with total cross sections of 17 (^{251}Fm) and 15 (^{252}Fm) nb. We obtained 19.7 nb (Al) and 83 nb (Au) for ^{256}Md . The ratio for the amounts stopped in the Al foils versus the Au varied with the isotope and ranged from 0.015 (^{252}Es) to 1.3 (^{252}Fm).

Since the main SF contaminant was determined to be 2.6-h ^{256}Fm coming entirely from the electron-capture (EC) decay of 77-m ^{256}Md , we further reduced its buildup by a factor of 3 to 4 by replacing the collection foils in SWAMI with fresh ones every 3 h. This prevented the growth of ^{256}Md and ^{256}Fm to saturation values during the course of the irradiations. Finally, our system was sensitive to counting only a sixth of the ^{256}Fm that decayed because the segment spanned by our detectors represents only that portion of the total circumference of the disk. The rate of formation of ^{256}Md was determined by two methods. One required only that we continue fission counting for a day after ending a bombardment to

measure the amount of longer-lived SF activity remaining on the foils. The other method was to irradiate for several hours and to collect all recoil atoms on a single foil centered behind the target. After turning off the ^{15}N beam, we rotated the disk to bring this foil between a detector pair, where it was counted for a day. From a number of such measurements, we established that the effective production rate of ^{256}Md was 1.3 times that of $^{260}[104]$. This production rate was used to correct each run on a set of foils for the number of fissions contributed by ^{256}Fm . Overall, ^{256}Fm accounted for 12% of the total fissions observed.

Before the resolution of the controversy concerning whether the half-life of $^{260}[104]$ was 80 or 22 ms, it had been suggested by Druin²⁵ that the 22-ms decay period measured at the Lawrence Berkeley Laboratory might be a composite of the 80 ms and a 14-ms period arising from the known fission isomer ^{242f}Am , possibly coproduced by a transfer reaction in bombardments of ^{249}Bk . Even though we could discount this possibility on other grounds, such as reaction energetics and the wholly different fission properties of the isomer,²⁶ we performed several experiments to detect the formation of 16-h ^{242g}Am . We established an upper limit of 50 nb for the formation of the ground state of ^{242}Am . This implies 20 pb would be an upper limit for making 14-ms ^{242f}Am based on the maximum ratio for the production of the fission isomer relative to the ground state of 4×10^{-4} (Ref. 27). It is certain from our cross-section limit that ^{242f}Am was not the source of any fissions in this study.

Although we had made a strenuous effort to keep the detection efficiency of SWAMI as high as possible, it was no larger than 5–6%. Major losses of 50% or more occurred because of decay of $^{260}[104]$ before reaching the first detector pair and after the fourth, a 30% counting geometry for coincident fragments, and the stopping of only a fraction of the recoils in the collector foils. We obtained five fission events from $^{260}[104]$ per hour of bombardment under the conditions noted above. In total, we observed 341 coincident fission events of which 41 were due to ^{256}Fm .

Because of the very low-event rate, we took a number of steps to eliminate erroneous fission pulses in the detectors and electronics caused by scattered ions from the beam, by radio-frequency (rf) noise, and by electrical discharges near the detectors from charge buildup. Aside from the usual precaution of supplying separate grounding for the electronics, we floated the detector bias voltages to the negative side, placed permanent magnets near each detector, encased the detectors with 3 mm of Pb shielding, and placed a Pb shield, with an open slot for the spinning disk, between the edge of the target and first detector pair. Radio-frequency noise would occasionally appear in bursts lasting from a few to 20 min, producing a large number of pulses over our discriminator thresholds of 20 MeV and rapidly filling our computer disk storage with false events. We found that each detector was acting as an antenna for rf emissions. We rejected this source of noise by configuring a fast majority-logic module to veto the digital output of our CAMAC analog-to-digital converters, when simultaneous pulses

from the detectors did not correspond to a pattern of just two pulses, with each coming from opposing detectors.

As a further precaution against accepting spurious pulses, we digitized and stored the time interval between the two pulses from each fission event. Using ^{252}Cf as an SF source, we determined that most coincident-fission pulses were within 2 ns of each other, while for a few events, this interval stretched to 40 ns as seen in Fig. 3. To account for these tails in the time distributions, we decided that fragments impinging near the edges of the detectors gave slow charge-collection times,²⁸ and therefore, longer time intervals between coincident pulses than those hitting the middle of the detector. This conclusion was reached after finding that the TKE distributions obtained from events with slower pulses were up to 6.3 MeV lower in energy than those from the main timing peak, implying that additional energy was lost by absorption in source and detector materials from fragments emitted at a low angle to the source plane. We accepted as valid coincidences all events with pulses that occurred within 40 ns of each other, but in addition, we applied a 1–2.9% energy correction to the ones whose timing fell outside the peak region in the time-interval distributions measured for each detector pair with ^{252}Cf .

Energy calibrations were made from specially constructed sources of ^{252}Cf . The ^{252}Cf was vacuum evaporated to produce a 9.5-mm-diam deposit on a $50\text{-}\mu\text{g cm}^{-2}$ Al foil, which was supported by the usual trapezoidal-shaped frame used in SWAMI. The Cf deposit was coated by evaporating an additional $57\text{-}\mu\text{g cm}^{-2}$ of Al metal over it to give a sandwich with a thickness closely equivalent to our normal $100\text{-}\mu\text{g cm}^{-2}$ Al collector foils. Calibrations were accomplished by replacing a frame on the disk holding the collection foils with one containing a ^{252}Cf source and by rotating the disk to bring the source in front of each detector pair for a fixed counting period. Calibrations were taken at the beginning and end of each run and about every 12 h during the runs to verify the electronic stability of the detec-

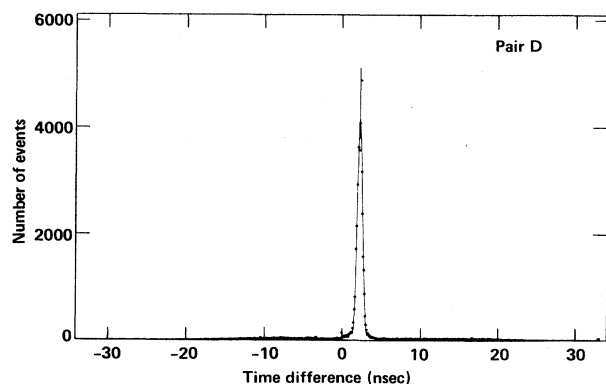


FIG. 3. Typical spectrum of intervals between arrival times of two correlated fission fragments using a ^{252}Cf SF source in SWAMI. The peak is slightly offset from zero due to small differences between cable lengths and to input/output delays in the two separate signal-processing channels.

tors and amplifiers. Using sets of energy calibrations nearest to the collection time of the $^{260}[104]$ data, we calculated fragment energies for each event from their pulse heights by the formula of Schmitt, Kiker, and Williams²⁹ together with the latest parameters given by Weissenberger *et al.*³⁰ Because the masses of the fragments are required for determining pulse-height defects, and since these are unknown initially, we used a successive iteration procedure that starts with the very approximate masses given by the inverse ratio of the pulse heights and proceeds to convergence by recalculating new masses and corrected pulse-height defects. It should be realized that the average TKE newly adopted for ^{252}Cf is 181 MeV,³⁰ a value 1–2% lower than the 183.1 and 184.1 MeV used previously.²⁹ Accordingly, our TKE's are not quite on the same energy scale as those measured earlier for other nuclides.

B. 1.2-ms ^{258}No

Given the very short half-life, this was another nuclide whose SF mass and energy division required the SWAMI apparatus for their investigation. Prior information was limited to a report noting its discovery as a 1.2-ms SF activity.³¹ Alpha-particle decay was not found by these researchers. This fission activity was observed in bombardments of ^{248}Cm only with ^{13}C ions and not with ^{12}C or ^{11}B ions. Bombardments of a ^{246}Cm target with ^{13}C ions also failed to produce this nuclide.

We have produced an activity with a half-life of 1.2 ± 0.2 ms (Fig. 4) by bombarding a ^{248}Cm metal target with 67.6-MeV ^{13}C ions from the 88-in cyclotron at the Lawrence Berkeley Laboratory. Most of our data were collected at beam intensities averaging 4.8×10^{12} particles/s. Assuming a 5% efficiency for SWAMI, we obtained a 17–18 nb cross section for the formation of what we believe to be ^{258}No . The target, in a 6-mm-diam deposit, was prepared by sublimation of 0.202 mg cm^{-2}

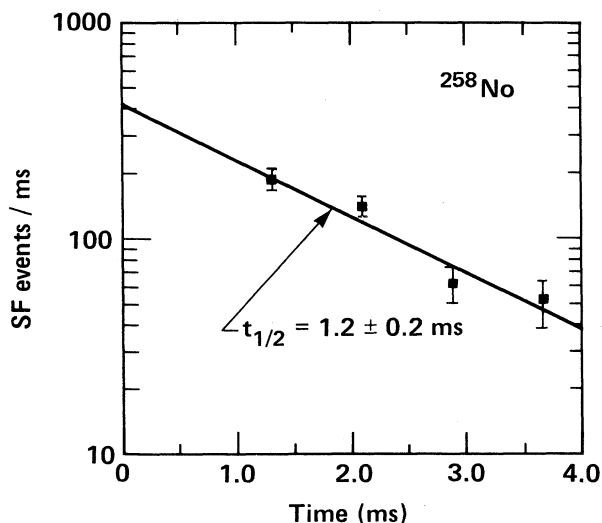


FIG. 4. Half-life of ^{258}No obtained from the four detector pairs in the SWAMI instrument.

of ^{248}Cm metal onto a 2.64 mg cm^{-2} Be backing foil.³² The Cm metal was then overcoated with $20 \text{ } \mu\text{g cm}^{-2}$ of Pd to prevent ejection of molecular clusters of curium during bombardment. Without this overlayer of Pd, we had found as much as 0.01% of the target isotope was being transferred to surfaces behind the target over an extended time period. In the case of ^{248}Cm , any transfer to the SWAMI collector foils would have created a background of long-lived SF activity.

A series of runs was made in which we varied the beam energy, rotation velocity, and thickness of the degrader foils used to reduce the energy of the recoils. The purpose was to determine if the 1.2-ms fission activity was the only short-lived one present and if its production and recoil characteristics were consistent with a compound-nucleus reaction. We found that the production rate of the 1.2-ms activity decreased by more than half when the beam energy was increased from 67.6 to 83.8 MeV. Upon increasing the degrader-foil thickness from 75 to $150 \text{ } \mu\text{g cm}^{-2}$ of Al, the yield of the 1.2-ms activity decreased by over 60%, and went to nil when the thickness was increased to $223 \text{ } \mu\text{g cm}^{-2}$. No ^{256}Fm was found with the thickest degrader foil at either ^{13}C ion energy. We had calculated that the maximum range of recoiling atoms of ^{258}No was $170 \text{ } \mu\text{g cm}^{-2}$ of Al. Thus, all of these observations are generally in agreement with a compound-nucleus reaction.

In the main, we set the rotation rate of the disk between 3606 and 3780 rpm, but four additional rates, each progressively slower, were tested to check for other fission activities with somewhat longer half-lives. These were 1963.6, 971.7, 257.8, and 23.12 rpm, which correspond to a point source passing by a detector pair in 1.49, 3.01, 11.3, and 126.3 ms, respectively. The number of fissions/mC, after subtracting an average of 0.052 fissions of ^{256}Fm /mC, dropped with rotation rate from an initial value of 0.361 to 0.28, 0.075, ~ 0.006 , and ~ 0.0 , respectively. These data demonstrated that, aside from 2.63-h ^{256}Fm , only a single, short-lived component was contributing to the observed fission activity.

We collected a total of 441 SF events during these experiments, 59, or 13%, were due to ^{256}Fm background for a net of 382 events from ^{258}No . We estimated from the growth and decay curves obtained for ^{256}Fm that nearly all of it was directly produced in transfer reactions rather than through the path of ^{256}Md EC decay. The amount of ^{256}Fm counted in each run from a set of collector foils was calculated from the measured production rate. Except for the points just discussed, the experimental parameters, energy-calibration methods, and measurement of the ^{256}Fm contribution were much the same as described above in our account of the $^{260}[104]$ SWAMI experiments. Because of the smaller recoil energy, we used degrader foils of $75 \text{ } \mu\text{g cm}^{-2}$ of Al for all production runs.

C. $370\text{-}\mu\text{s}$ ^{258}Fm

Since the discovery of this isotope in a rotating-drum experiment,³³ its mass and atomic numbers have been confirmed and the original half-life of 380 μs has been

modified slightly.³⁴ In the discovery experiments, this isotope was produced by the $^{257}\text{Fm}(d,p)$ reaction, but subsequently it has been made in neutron irradiations³ of ^{257}Fm and as the daughter of the 60-min isomer of ^{258}Md .^{4,35} Both the excited-state fission and SF properties had been investigated earlier in measurements disturbed by poor energy resolution and, for the SF study, subtraction of a large ^{256}Fm SF component amounting to 65%.^{3,4} Largely because of the amenable half-life of its Md parent and our capability of producing ^{258m}Md in appreciable amounts from heavy-ion bombardments of ^{254}Es , we have been able to explore the fission properties of ^{258}Fm with much greater precision than before.

We prepared ^{258m}Md for fission studies of its daughter by bombarding 276-d ^{254g}Es with 105-MeV ^{18}O and 126-MeV ^{22}Ne ions. Beam intensities over an illuminated area 3 mm in diameter ranged from 1.2 to 1.7×10^{12} particles/s⁻¹. Cross sections for transfer reactions producing the isomer from ^{18}O and ^{22}Ne were 43 and 55 μb , respectively, values that are approximately one-third of those for making the nonfissioning, 53-d ground state of ^{258}Md .³⁶ The target was made by electroplating 3.34 μg of ^{254}Es onto a 4.5 mg cm⁻² Mo backing foil. The Es deposit was 3 mm in diameter, which gave an initial areal density of 47.2 $\mu\text{g cm}^{-2}$. This deposit was overcoated with 15 $\mu\text{g cm}^{-2}$ of Pd metal, but as a further precaution against transfer of ^{254}Es , we mounted a 50- $\mu\text{g cm}^{-2}$ Al foil 2 mm behind the target. Nuclei recoiling from the target passed through this thin cover foil, and were caught on a 3.6 mg cm⁻² Ta foil positioned about 8 mm behind the target. This target and subsequent ones of ^{254}Es were placed in the same vacuum chamber and target system used in the SWAMI experiments. However, because of the greatly increased radiation hazards associated with ^{254}Es , additional interlocks to the cyclotron and vacuum systems were installed to prevent catastrophic failure of the targets that might be caused either by our own errors or by system malfunctions.

Following each bombardment, we isolated ^{258}Md / ^{258}Fm from the other reaction products by off-line mass separation. Mass separation was vital in reducing, to a nearly negligible level, the potentially overwhelming SF interference from ^{256}Fm and for ensuring that our fission measurements were being made on a single nuclide. From ^{22}Ne reactions, ^{256}Fm is produced with a 840- μb cross section, but its persistence is supported by EC decay of 76-min ^{256}Md and β^- decay of 7.6-h ^{256}Es that are coproduced with two to six times larger cross sections.³⁶ Immediately after the end of a bombardment, the Ta catcher foil was removed from the SWAMI vacuum chamber and flown ~ 60 km by helicopter from the Lawrence Berkeley Laboratory to our laboratory, where the mass separation took place. The foil retaining the recoil products was inserted into a tungsten crucible used in the surface-ionization source of our mass separator. At the collector end of the mass separator, we attached a partially masked, 13-mm-diam support ring covered with 50 $\mu\text{g cm}^{-2}$ of Al to a 56-cm long, rectangular Al backing foil. This backing foil was placed in the horizontal focal plane of the separator with the ring centered at the anticipated $A=258$ mass position. Masses adjacent to 258

were stopped in the backing foil. The horizontal separation between each mass unit was 13 mm, which allowed a span of 10 mass units to be collected simultaneously on the foils. After about 15 min of mass separation, the foils were quickly recovered, and the locations of easily identified mass markers, ^{254}Fm and ^{256}Fm , were verified by scanning the backing foil with an α counter. Because of time urgency, our first judgment concerning the mass resolution and mass locations on the foils was based on this initial α scan: afterwards, we autoradiographed the larger Al foil to determine these factors accurately. We later discarded fission data from one run with ^{18}O ions because the 258-mass fraction was not centered within the designated ring. The ring supporting the 50- $\mu\text{g cm}^{-2}$ Al foil with the mass-258 deposit was detached from the larger Al foil for insertion into a coincident-fission counter. Our overall efficiency determined for the mass-separation process varied from 20 to 30%.

We measured the energies of correlated fission fragments in a high-geometry counter consisting of two surface-barrier detectors mounted face to face in a vacuum chamber with a 2-mm gap between them for insertion of the sample. The average geometric efficiency was 61% for coincident fragments. For the purpose of simultaneously detecting β^- decay in another experiment, the depletion depth of these detectors was 1 mm. Their energy resolution in terms of full width at half maximum (FWHM) for 5.49-MeV α particles from an ^{241}Am source was 15.8 and 14.9 keV. The slower, analog fission pulses were gated into CAMAC digitizers by a slightly delayed logic pulse generated by constant-fraction discriminators whose inputs came from the fast-pulse outputs of the preamplifiers. A coincidence module was unnecessary because both fragment pulses were accepted with a single gate pulse of 1.2- μs width. For each event, we stored the energies recorded for two fragments and the clock time derived from a 1-kHz pulse generator.

Calibrations of the detectors were made with SF sources prepared by high-temperature vaporization of ^{252}Cf onto Al foils that were masked to give a 9.5-mm-diam deposit. The foil thickness was the same as the source foils from the mass separator. To prevent self-transfer of ^{252}Cf fission activity to our detectors, we overcoated the Cf surface with 50 $\mu\text{g cm}^{-2}$ of Al. Later, it was necessary to make an energy correction of 3.2 MeV to the ^{258}Fm fission fragments entering the upper detector because of the additional energy loss in the calibrations due to ^{252}Cf fragments passing through this extra layer of Al. This calculated value for the loss was authenticated by establishing that the average fragment energy for ^{258}Fm was the same in each detector within 0.6%. The procedure for converting pulse height to energy was identical to the one described for $^{260}\text{[104]}$.

From two bombardments with ^{22}Ne ions, lasting 202 and 375 min, we obtained 1570 SF events. The elapsed times from the end of the bombardments to the start of counting for these two runs were 63 and 66 min. We fission counted for over 1200 min in each experiment, but events beyond 300 min in one and 350 min in the other, were excluded from our final list to minimize the contribution from longer-lived ^{256}Fm that was supported main-

ly by its parent, 7.6-h ^{256}Es . Of these 1570 events, we attribute 108 to a mass-256 adulteration caused by scattering of ions in the mass separator. This number of ^{256}Fm fissions was obtained from least-mean-squares analysis of the fission-decay curves.

D. 100-min ^{259}Md

Decaying primarily by SF, this isotope was first found as the product of EC decay by 59-min ^{259}No (Ref. 37). The branching ratio for EC by ^{259}No was found to be $25 \pm 4\%$, the remainder being α decay to ^{255}Fm . Taking advantage of this appreciable branching ratio and a unique divalent ionic state of No that allowed rapid chemical separations from other reaction products made in the bombardments, we first produced quantities of chemically isolated $^{259}\text{No}/^{259}\text{Md}$ sufficient to determine the mass and fragment-energy distributions and the emission of light charged particles accompanying the SF of ^{259}Md .³⁷ The mass division was decidedly symmetrical, whereas the average TKE was found to be 201 MeV, about 35–40 MeV lower in energy than the average for ^{258}Fm and ^{259}Fm . Based on Coulomb repulsion arguments, these low-fragment energies seemed incompatible with mass symmetry giving spherical Sn-like products. At the time of publication of Ref. 37, we suggested the charge centers of the emerging fragments must be further apart and, therefore, that the ^{259}Md nucleus is more deformed at the scission configuration than ^{258}Fm and ^{259}Fm nuclei. Inconsistent as the picture was, we still failed to perceive that these findings might indicate an entirely new fission mode.

These results from our earlier fission studies have been superseded by the measurements reported here on mass-separated samples of ^{259}Md . Sources prepared by ion implantation in the mass separator were thinner, and provided much superior energy resolution for fission fragments when compared to the ones made earlier by evaporating aqueous solutions. Moreover, we could produce many more atoms of ^{259}Md directly from transfer reaction than indirectly through the production of ^{259}No followed by EC decay.

Our production, mass-separation, and fission-counting methods were identical to those described for ^{258}Fm . We produced ^{259}Md with 4.5- μb (126-MeV ^{22}Ne) and 7.2- μb (105-MeV ^{18}O) cross sections in bombardments of ^{254}Es . Although four bombardments were made, we have not included the data from two of them because poor mass-separator resolution resulted in ^{256}Fm - ^{258}Fm SF activities contributing up to 31% of the total fissions. Counting of fissions extended to 1 d or longer, but events occurring after 420 min in one run and 500 min in the other were excluded to keep the ^{256}Fm contribution small. From the two best experiments, we obtained a total of 500 coincidence events, of which we credit 50 to ^{256}Fm and ^{258}Fm as mass contaminants. The amount of ^{256}Fm was determined by resolving the components of the gross fission-decay curve, whereas the 11 events we attribute to ^{258}Fm were determined from the amount of ^{258m}Md in the samples at the start of counting. By measuring the α -decay rate of 53-d ^{258g}Md in the mass-259 samples and from

measuring the ratio of the isomer to ground state in the mass-258 fractions, we established the quantity of ^{258m}Md in the mass-259 samples coming from incomplete mass separation.

E. 32-d ^{260}Md

We recently discovered this long-lived isotope of Md in mass-separated samples during the course of investigating the products of transfer reactions originating from heavy-ion bombardments of ^{254}Es .^{1,35} The atomic number was verified by chemical methods, and the mass number was defined by electromagnetic isotope separation. Initially, we considered the observed SF activity might well come from either ^{260}No or ^{260}Fm daughters because of favorable estimates of Q values for β^- or EC decay by ^{260}Md . These daughters are expected to have subsecond SF half-lives, allowing them to be in secular equilibrium with the much longer-lived parent. We have since determined by the method described in Ref. 34 that branching ratios for possible decay modes in ^{260}Md (β^- , K -electron capture, and L -electron capture) are each no greater than 10%, provided the daughter half-lives are 100 ms or less.^{1,38} Thus, we are assured that most if not all of the SF activity we observed in the mass-260 fraction emanates directly from ^{260}Md .

Our experimental procedures for measuring the fission properties of ^{260}Md from one set of samples were the same as those employed for ^{258}Fm and ^{259}Md . Namely, we produced this isotope in 8- to 12-h bombardments of ^{254}Es with either ^{18}O or ^{22}Ne ions. The formation cross section was about 300 nb for either projectile. From two bombardments followed by mass separation, we obtained 531 correlated SF events in the mass-260 fractions, with none arising from isotopes other than ^{260}Md . By delaying the start of fission counting for several days after a bombardment, we eliminated the shorter-lived Fm and Md SF emitters as contributors to our fragment-energy measurements. Also, we confirmed that longer-lived SF activities were not present by tracking SF decay in the samples for up to 6 months in high-efficiency ionization counters.

In addition to these 531 events, we obtained another 903 events of ^{260}Md from a single source that was fission counted during neutron-multiplicity measurements at Philipps University, Marburg, Federal Republic of Germany.¹⁴ This sample came from chemically isolating Md from many recoil-collection foils containing reaction products from a series of ^{22}Ne bombardments of ^{254}Es . The ^{260}Md was recovered as a by-product of other experiments aimed at studying new isotopes of Lr.³⁹ The chemically purified Md was electroplated onto a 27- $\mu\text{g cm}^{-2}$ film of polyimide that had been coated on one face with 50 $\mu\text{g cm}^{-2}$ of vacuum-evaporated Au. Electroplating produced a thin deposit 4.0 mm in diameter. A ^{252}Cf calibration source was prepared identically at the same time. At the start of fission counting, our final sample of Md contained about 15 times as many atoms of 53-d ^{258}Md as ^{260}Md because, unlike our previous samples, Md had not been mass separated. Nevertheless, with a SF half-life greater than 4700 yr (Ref. 40), ^{258}Md constituted a negligible source of fissions. The sample of ^{260}Md was

mounted in a vacuum chamber between two 450-mm² surface-barrier detectors located in the center of a neutron-detection tank, and fission counted for 98 d. To avoid contaminating the detectors with ^{252}Cf , the energy response of these detectors was calibrated with fission fragments from our ^{252}Cf source after we finished the ^{260}Md counting. We calculated fragment energies by the same procedure described earlier, and combined these events with the previous ones.

III. RESULTS

A. Mass and energy distributions

We present in Figs. 5 and 6 the mass and TKE distributions obtained for the five nuclides after subtracting background distributions contributed by small and known amounts of ^{256}Fm . This correction was made by scaling downward the distributions we obtained from 250 000 events collected from a mass-separated sample of ^{256}Fm to equal the total number of ^{256}Fm events we found in our sources. The ^{259}Md distributions were also adjusted for the 11 events coming from a ^{258}Fm impurity. As noted in the previous section, no background corrections were necessary for ^{260}Md . Unlike most previous studies where ^{256}Fm was a major fission component, we found that subtracting the contribution from ^{256}Fm had only a slight impact on any distribution.

For the reason that we recalculated our fragment energies from the more recent calibration parameters for ^{252}Cf (Ref. 30), the histogram distributions shown in Figs. 5 and 6 do not quite correspond to those given in Ref. 1. Another difference is that we have nearly tripled the number of observed fission events from ^{260}Md since the publication of Ref. 1.

The most significant and unique feature of the TKE distributions is their pronounced deviation from a single Gaussian shape. In four of the five nuclides, decided asymmetry is imparted by conspicuous tailing in either energy direction from the central peak. This is the first observation of this phenomenon, the TKE distributions from other actinides being uniformly Gaussian with only minor divergences. Detection of this feature was made possible by reducing the interference from the SF of ^{256}Fm and improving the fragment-energy resolution over that of our earlier work. Closer inspection of these TKE distributions reveals that the peak of each distribution is not randomly located along the energy axis, but is positioned near either 200 or 233 MeV. The asymmetric tails of the TKE curves result in distributing an appreciable portion of the events into one or the other of these two main energy regions.

Based on these observations, we considered that the TKE curves for at least four of the nuclides were a composite of two separate energy distributions, with each most likely being Gaussian. The fifth, $^{260}[104]$, may well have a residue of the high-TKE component, but we cannot be sure because of the statistically few events in the high-energy region. By taking the FWHM from the TKE distribution for $^{260}[104]$ as a fixed parameter and model for the lower-energy Gaussian, we resolved each of

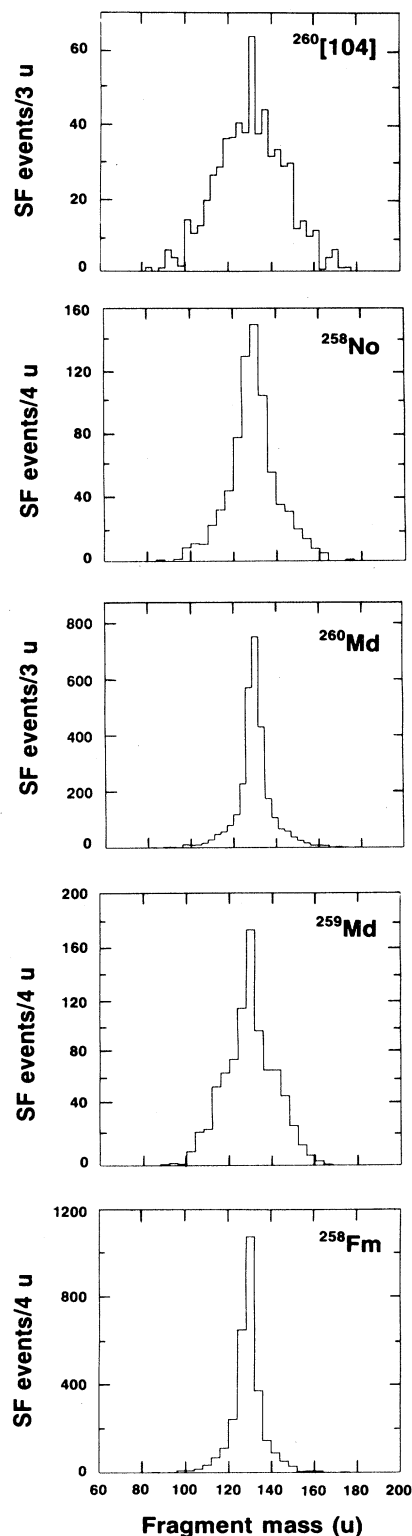


FIG. 5. Provisional mass distributions (no neutron corrections) obtained from correlated fragment energies. The mass bins have been chosen to be slightly different for each nuclide. The distributions are net after subtracting a small ^{256}Fm component.

the gross TKE distributions from ^{258}Fm , ^{258}No , ^{259}Md , and ^{260}Md into two Gaussian distributions by least-mean-squares fitting. The results are shown in Fig. 7. Reduced- χ^2 values resulting from the fitting of two

Gaussians, together with the centroids of the TKE's and percentage abundances of the low- and high-energy peaks, are given for the four nuclides in Table I. Because the reduced chi-squared values are near unity, the fitting of two Gaussian functions appears to be a good approxi-

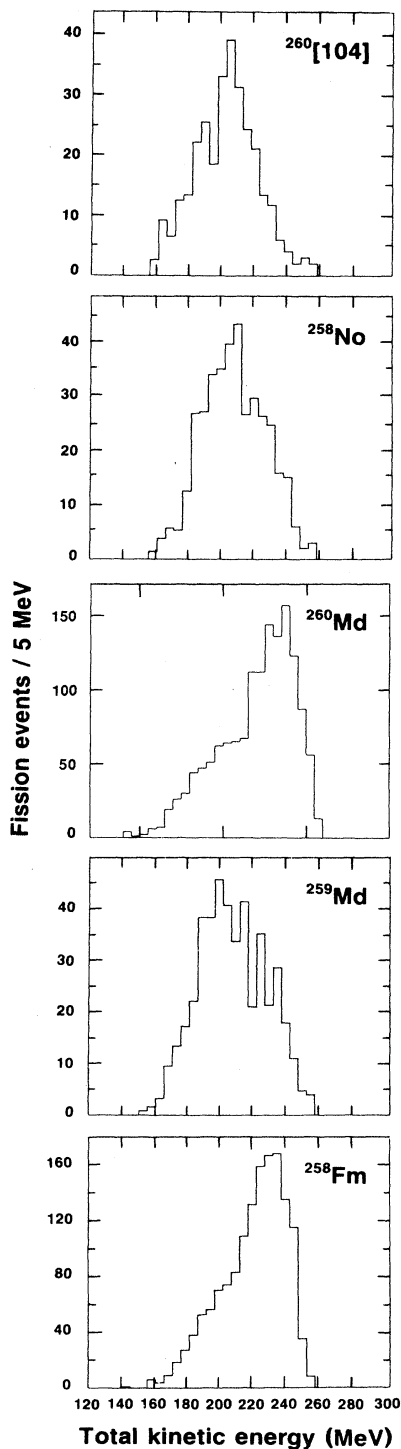


FIG. 6. Provisional total-kinetic-energy distributions. A small contribution equivalent to the known amount of ^{256}Fm has been subtracted from all but the ^{260}Md distribution.

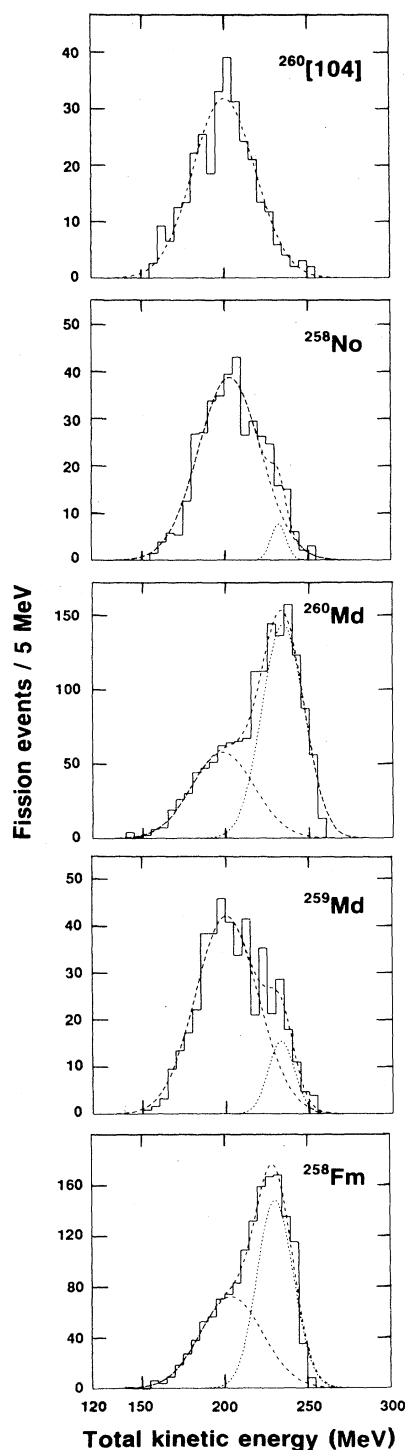


FIG. 7. Unfolding of the asymmetric TKE distributions of Fig. 6 into two Gaussians by least-mean-squares fitting.

TABLE I. Parameters obtained from least-mean-squares fitting of two Gaussians to the TKE curves. Reduced χ^2 is a measure of the quality of fit, where values from 0.5 to 1.5 indicate a reasonable probability of a good match.

Nuclide	Low-energy		High-energy		Reduced χ^2
	peak (MeV)	Abundance (%)	peak (MeV)	Abundance (%)	
^{258}Fm	205	50	230	50	1.32
^{258}No	204	95	232	5	0.52
^{259}Md	202	88	234	12	0.81
^{260}Md	200	42	234	58	1.10
$^{260}\text{[104]}$	200	100			0.63

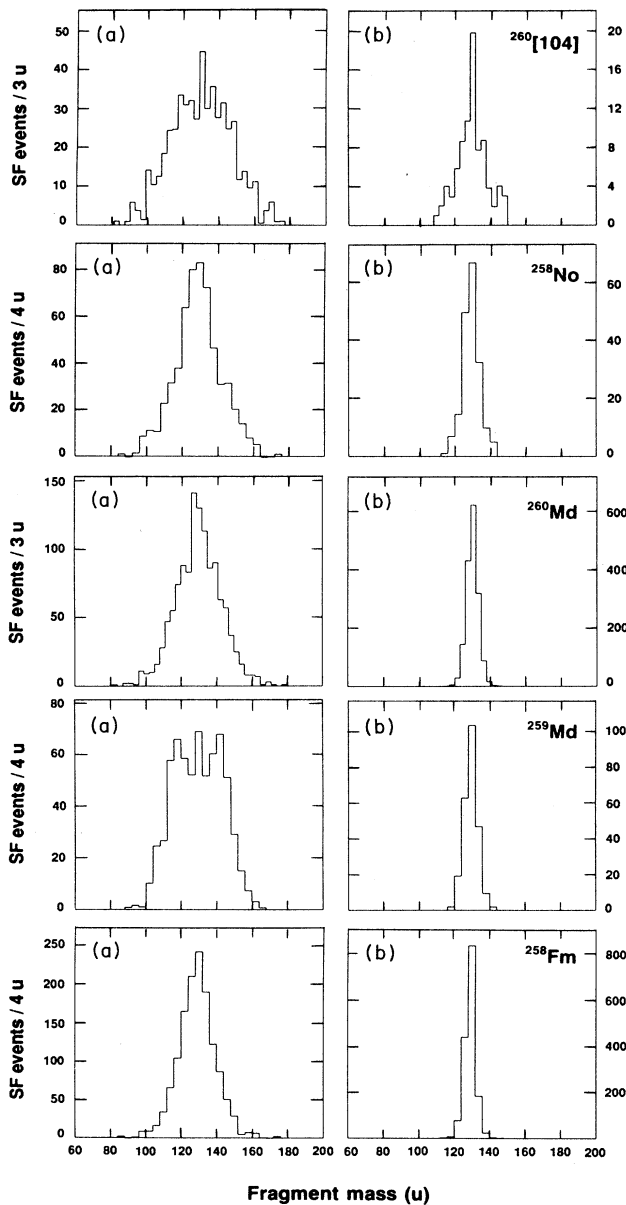


FIG. 8. Mass distributions obtained by sorting fission events according to their total kinetic energies: (a) for events with TKE's < 220 MeV and (b) for those with TKE's ≥ 220 MeV.

mation to the parent distribution. Probable errors range from 1 to 2 MeV in the peak locations and an absolute 2–3% in each of their abundances. Although the extraction of two Gaussians by this analytical approach is highly suggestive of such a composite, it should not be construed as proof.

Our mass distributions shown in Fig. 5 are all symmetrical, with the FWHM ranging from 7.9 u for ^{260}Md to 36 u for $^{260}\text{[104]}$. It is apparent that nuclides having the narrowest mass distributions also have a preponderance of high-TKE events. Conversely, the very broad mass distribution found for $^{260}\text{[104]}$ is associated with a single TKE peak with a low energy. These obvious correlations with TKE are further reinforced when we plot the mass distributions from events sorted by their TKE's. Arbitrarily choosing 220 MeV as the dividing line between the low- and high-TKE peaks, we show in Fig. 8 the mass distributions obtained after sorting events into bins lying above and below this energy. We find it remarkable that the high-energy mode of fission consistently produces such narrowly symmetrical mass distributions as found in these nuclides. Given this singular behavior, it is difficult to escape the conclusion that, for this fission mode, the process is guided toward these mass divisions by the proximity of the fragments to the closed shells in ^{132}Sn . While still symmetrical, the mass distributions for events with TKE's less than 220 MeV are much broader, spanning over twice the mass range of those from the high-TKE mode. It is these lower-energy events that are responsible for the wings of the main peaks, extending far outward in mass, that we see in Fig. 5 for most of the nuclides. If we choose SF events with TKE's less than 200 MeV, the mass distributions become even broader and are nearly flat but remain symmetrical, with the exception of ^{258}Fm and ^{259}Md , which revert to asymmetrical distributions. Thus, the gross differences seen in the mass distributions from events binned by energy clearly add another distinctive trait that separates the low-energy mode from the high-energy mode of fission.

B. Isotopic assignments

Briefly setting aside our discussion of the fission results, we wish to first appraise the soundness of the isotopic assignments for the five nuclides studied. As noted in the experimental section and the references provided therein, the atomic and mass numbers of ^{258}Fm , ^{259}Md ,

and ^{260}Md have been firmly established. This is not the case for ^{258}No and $^{260}[104]$, since their Z and A values have been inferred from the nuclear reactions, where they have and have not been successfully produced, and the energetics and kinematics of these reactions. The sum of this evidence heavily favors these isotopic assignments because it is consistent with compound-nucleus reactions, and because the possibilities of alternative assignments have nearly vanished after years of exploring this region of nuclides. At first, the 17-nb cross section for producing ^{258}No from the $^{248}\text{Cm}(^{13}\text{C},3n)$ reaction seemed exceptionally small to us when compared to an expected value of 170 nb calculated by the JORPLE program.⁴¹ Nevertheless, our cross section appears reasonable when compared with the 6-nb cross section found in the similar $^{249}\text{Cf}(^{13}\text{C},3n)^{259}[104]$ reaction.⁴² The JORPLE program indicated 21 nb for this reaction. In addition to these arguments, the mass and TKE distributions from the SF of ^{258}No and $^{260}[104]$ are unique to the SF of the neutron-rich transeinsteinium isotopes, and are unlike even those we report for nearby nuclides. Considering our knowledge of how these nuclides are produced and decay, we believe the sum of this information points to the correctness of their isotopic assignments.

IV. DISCUSSION AND CONCLUSIONS

We have investigated enough nuclei in this region to comment on trends in fission properties, on the underlying causes of these uncommon modes of fission and, above all, on direct observation of bimodal fission and its relevance to advancing our fundamental understanding of the fission process. Even though we can make several important qualitative connections to theory, we conclude that theory has serious weaknesses in explaining other features that we see. Based on one such connection, our results imply that the low-energy mode of fission we observe will likely extend to far heavier nuclei, well beyond the five studied so far. We can state that symmetrical mass division and high TKE's are no longer unique to just ^{258}Fm and ^{259}Fm . Our results from these five nuclides show that all fission symmetrically and that four of the five have a significant component with high TKE's. The concept of this being a small islet of symmetrical fission emerging for a singular reason should now be rejected.

We suggest that two different fission modes are separately responsible for distinctive regions of the TKE distributions displayed in Fig. 6. In four of the five nuclides reported here, we find anomalous TKE distributions, skewed in energy sufficiently to be easily describable by two Gaussian distributions. Asymmetrical tailing from the peak energy occurs toward either higher or lower energies. Furthermore, we find that the peak in each of the gross TKE curves falls in one of two distinct positions, either near 200 or near 233 MeV. When resolved into two Gaussian distributions, the constituent peaks also lie very close to these same two energies, as shown in Fig. 7. We find the division of mass to be symmetrical for every nuclide studied; however, very sharply symmetrical mass distributions are correlated with events belonging to the

high-energy mode of SF. The low-energy mode is marked by broadly symmetrical mass distributions, as portrayed in the SF of $^{260}[104]$. From these distinguishing features, we conclude there are two distinct modes, or bimodal fission.

Because our TKE distributions are wholly unlike those for lighter nuclei, we believe it is necessary to offer an explanation. Our analysis of the TKE distributions tells us they are composed of two distributions with very different Coulomb repulsion energies. By necessity, the high-energy mode is compact and spherical at the scission point, whereas the low-energy mode must be highly deformed and elongated when the fragments separate. We can account for the high-energy mode on the basis of fragment shells that are emerging between the saddle and scission point.¹³ As noted in the Introduction, fragment shells near the doubly magic ^{132}Sn lower the potential-energy path and, thereby, favor the mass division into spherical Sn isotopes near the 82-neutron closed shell. As N decreases below 158 neutrons and Z of the fissioning species increases beyond 100, the opportunity to divide into two fragments near these magic proton and neutron numbers diminishes. Thus, we observe a trend away from the spontaneous-fission mode, characterized by unusually high TKE's and toward the low-energy mode represented by $^{260}[104]$.

An equally satisfying explanation for the low-energy mode is less apparent. Lacking a credible alternative, we are persuaded to believe its appearance is associated with the dropping of the second fission barrier below the ground state. This event is predicted to commence in the same Z and N space as for fragmentation into near magic nuclei. Theorists have determined that the second or outer fission barrier is lowered by 0.5–2 MeV when shapes from asymmetric deformations are included in their calculations of potential-energy surfaces (PES).⁴³ This lower energy path on the PES may be responsible for the asymmetrical mass distributions found in all but the heaviest actinides.⁴³ On the other hand, the inner barrier favors reflection-symmetric shapes, being stiff toward any asymmetrical deformations. Upon the disappearance of the second barrier below the ground state, passage through the remaining inner barrier should qualitatively yield symmetrical mass distributions and TKE values that conform to those expected of liquid-drop fission. For the low-energy mode, our average TKE of 200 MeV and the broadly symmetrical mass and TKE distributions are entirely consistent with those expected from liquid-drop fission. Our TKE's for the low-energy mode are compared in Fig. 9 with the TKE systematics for liquid-drop fission. The lines, from Viola *et al.*⁴⁴ and Unik *et al.*,⁴⁵ define the best fits to experimental liquid-drop TKE's for a much broader range of nuclei.

It would not be too surprising to find this mode of fission if the barrier were due solely to liquid-drop potential energies. It is a well-known property of the liquid-drop model to produce a single barrier with a strong preference for reflection-symmetric shapes. However, the barriers for our nuclides are largely built from single-particle couplings rather than from liquid-drop energies.⁶ Even so, mass-symmetric shapes before the second saddle

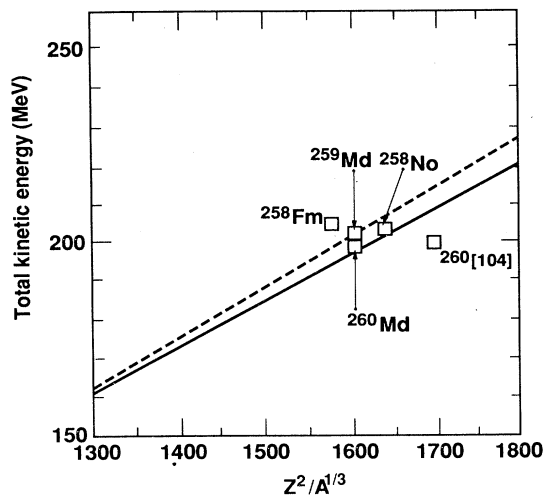


FIG. 9. Comparison of expected liquid-drop TKE's (lines) with the TKE's obtained for our low-energy mode of spontaneous fission. The lines are defined by the best fit of experimental TKE's to a linear dependency on the Coulomb parameter, $Z^2/A^{1/3}$ in the liquid-drop model of fission. The solid line is given by Viola *et al.* in Ref. 44. Dashed line is from Unik *et al.* in Ref. 45.

are clearly preferred throughout this region of heavy nuclei.⁹ Therefore, no matter how the first barrier is constituted, we would expect the resultant fission behavior to be roughly the same. Essentially, our observation of liquid-drop fission properties for $^{260}[104]$, in which the liquid-drop portion of the barrier is only about 15%,⁶ indicates experimental verification of this hypothesis. To produce the broad spread observed in these mass distributions, we presume that in the descent from the first saddle to scission, factors associated with collective motions will cause a sizable redistribution of mass between the two emerging fragments.

The explanations we offer for each mode of bimodal fission are based upon very general features previously established by PES calculations for static deformations. Each mode is derived from the effects of shell structure; one in the parent fissioning nucleus and the other from single-particle couplings in the fragments. How each can coexist and occur with near equal probability in the same nucleus presents a challenging problem that, so far, remains unsolved. Originally, we had mentioned that the mapping of two distinct paths on the PES, separated by a ridge at the later stages to prevent reequilibration during the descent to scission, was necessary to accommodate our results.¹ Theorists responded broadly and generously to this suggestion and have, indeed, found appropriate paths on the PES.^{46,47} We refer the reader to the cited references for views of these new valleys in the PES landscape. Still, all is not well with the current picture because there has been no physical grounds advanced that would allow near-equal populations to traverse each path. We would liken the requirement to having a traffic policeman standing at the juncture of the two routes after the second saddle and directing about equal numbers along each. In one attempt, Möller *et al.* has estimated

that the inertial masses for compact shapes are considerably less than those in the trajectory taken by the elongated mode.⁴⁷ The consequence is a much higher rate towards scission for nuclei traveling the less-deformed route; hence, the probability for taking this path is enormously increased. Of course, this clearly violates our measured ratios for the relative populations. We strongly suspect that dynamical aspects govern the choice of routes, but the capability to solve the dynamics when combined with microscopic features does not yet exist.

The concept of two fission modes, characterized by their mass distributions, appeared many years ago when Turkevich and Niday suggested that there are two fundamentally different modes by which fission may proceed.⁴⁸ One mode supposedly predominates at low-excitation energies and the other at high-excitation energies, with the relative proportions changing with excitation energy. In their purest form, the two modes led to either a symmetrical or an asymmetrical mass distribution. Over the intervening years this suggestion has resurfaced,^{49,50} only to be discounted because of the lack of sufficiently clear evidence. However, the two modes we report are unrelated to the ones proposed by Turkevich and Niday. Ours are likely due to a coincidence in which favorable shell structures in the fragments *and* the fissioning nucleus occurs within the same select group of nuclei. Excitation energy is a curse to the modes we suggest since shell structure is destroyed as internal excitation increases.

In contrast to the lighter actinides, where the differences in fission properties from one isotope to the next are subtle and nearly imperceptible, we find the addition of a single nucleon results in abrupt and striking changes in the TKE and mass distributions. Adding a proton to ^{258}Fm causes the high-TKE mode to recede sharply in ^{259}Md , and the addition of a neutron to the latter nuclide brings about a sudden return of this mode in ^{260}Md . On the other hand, there seems to be little change in the extent of the high-energy mode in the transition from ^{259}Fm to ^{260}Md . Within this group of four nuclides having values of $N \geq 158$, the SF properties of ^{259}Md appear to be at odds with those of its three neighbors for reasons that we assume can be delegated to its Nilsson structure. The alternative of assigning a predominant role to fragment properties in the case of ^{259}Md is difficult because there should be little difference in the fragments from this nuclide compared to those from the SF of its neighboring nuclei, ^{258}Fm , ^{259}Fm , and ^{260}Md . A further example of the erratic behavior of fission properties for nuclei in this region is the nonsystematic variation of SF half-life with Z and N . It is recognized that SF half-lives reflect shifts in ground-state shell corrections when Z and N of the initial nucleus are varied. Also, a thinning of the fission barrier, which can suddenly shrink with increasing Z or N due to the disappearance of the second or outer hump of the two-humped barrier, can be responsible for precipitous half-life reductions.⁷ Such sudden changes in the end results of the fission process appear to reflect a strong coupling of the collective motions with the intrinsic internal structure of the nucleus during deformation. Furthermore, dynamical as-

pects of fission, e.g., inertial mass, can be strongly affected by bunching and debunching of the Nilsson levels as the nucleus deforms. These notions require the fission process to be adiabatic.⁵¹

Because macroscopic forces are expected to vary smoothly with Z and N , we are compelled to conclude that the sharp changes in fission properties from nuclide to nuclide are due to shell effects. Clearly, single-particle couplings in the fissioning nucleus and its fragments play an even larger role in the fission process than we previously expected. However, all static models of fission based on the Strutinsky method tend to average contribution from the single-particle levels because of the Nilsson Hamiltonian and are, therefore, incapable of reproducing the abrupt changes in half-lives and fission properties that we observe experimentally. In any theoretical description of fission, we believe it is essential to include explicitly these parameters, which depend so strongly on Z , N , and deformation, rather than allowing them to average the level structure.

The north and east boundaries marking the Z and N region for which the high-energy mode of fission exists have not been determined experimentally. Exploration of the very neutron-rich region at the eastern limit may never be possible because the combination of targets and projectiles necessary to reach this area is unavailable. With respect to the southern and western borders, our current knowledge indicates that Fig. 1 in Ref. 9 provides a reasonable estimate of their location, provided a preponderance of the high-energy mode is required for their definition. Farther to the west, we observe a trend signaled by fading of the high-TKE mode together with broadening mass distributions when $Z \geq 102$ and $N \leq 156$. This conforms to our expectations in that there is a diminishing opportunity for division into two Sn fragments when Z of the fissioning species increases beyond 100. For example, the mass distribution for ²⁶⁰[104] is not nearly as sharply focused around mass 130 as it is for nuclides closer to Fm. However, if N increases, as in the Md isotopes, and approaches 164, the influence of the 82-neutron closed shell in the fragments again tends to enhance the high-energy mode of fission. The upward extent of Z in which the proximity to 164 neutrons influences fission properties is not yet defined, but we have evidence from fission studies of ²⁶²No that it persists into the heaviest No isotopes to nearly the same degree that we found for the neutron-rich Md and Fm isotopes.⁵² This finding is consistent with the forecast cited above in Ref. 9. We hesitate to speculate about the northern and eastern limits to this mode of fission, but would suggest that it will disappear as suddenly as it appeared, which is when strong fragment shells are no longer available. However, we believe it safe to venture that the combination of magic neutron *and* proton numbers in the fragments from the fission of ²⁶⁴Fm could lead to totally “cold fission” with exceedingly sharp TKE and mass distributions. By “cold fission,” we mean that virtually all of the energy available for the fission reaction (Q value) is removed by the kinetic energy of the fragments, leaving almost nothing for their internal excitation.

We presume that symmetrical mass division will be typical of SF throughout a region of the most massive nuclei that borders and includes those still undiscovered. We make this projection on the grounds that all PES calculations show the second barrier not only dropping below the first barrier but also completely vanishing for all nuclei with $Z \geq 106$, thereby providing what we believe to be the necessary basis for low-energy symmetrical fission to prevail. Mass asymmetry reported as probable for the SF of ²⁶²[105] seemingly challenges our prophecy.⁵³ However, the evidence for mass asymmetry from the fission of this nuclide is not strong when one considers that only 181 ± 51 fission events out of a total of 950 were due to ²⁶²[105], the rest coming from the SF of ²⁵⁶Fm. It seems somewhat questionable to us as to whether or not a meaningful mass distribution can be isolated from an overbearing asymmetrical one arising from ²⁵⁶Fm. In support of our expectation of a low-energy fission mode for this nuclide, the authors did not find any high-TKE events near 250 MeV, which would have been the signature of our high-energy mode.

This new region of low-energy, mass-symmetric fission reverses a trend that began in the preactinides where two modes of fission are also observed.² In the preactinides, one mode leads to mass-symmetrical division, with properties similar to our low-energy mode, whenever passage to scission is through or over a primarily liquid-drop barrier. However, the strengthening of shell effects as the actinides are approached causes the growth of a second or mass-asymmetrical barrier,⁵⁴ thereby producing an increasingly significant mass-asymmetrical component as a second fission mode. The ascendancy of the mass-asymmetrical barrier reaches its maximum in the early members of the actinide series and begins to fade thereafter. For neutron-rich nuclei near the end of the actinides, similar calculations of the PES suggest that the second, mass-asymmetrical barrier is rapidly shrinking with increasing Z and A ,^{7,9} a trend that presages the low-energy and mass-symmetrical mode of fission we observe.

In conclusion, we wish to note that fission theory appears to be lagging well behind experimental findings, whereas we would greatly prefer the reverse to be true. Rather than illuminating the way, theorists are attempting to reconcile their models with observations, a circumstance truly indicating we are, even after 50 yr, still at a rather early stage in our attempts to understand the fission process. As examples, most of the results and conclusions we report were unanticipated, even though much of the theoretical framework necessary for their prediction was in place. Half-life estimates for SF, with their 5–9 orders-of-magnitude uncertainty, offer almost no guidance to the landscape ahead in the search for new and heavier nuclides. Our foremost concern is this inability of the current static models to provide detailed predictions of fission properties. Perhaps we are expecting too much at this stage of development, but the ultimate value of theory lies in its ability to accurately forecast phenomena well ahead of their observation. After much discussion with theorists concerning the limitations of fission models based on the Strutinsky-Nilsson formulation, we have arrived at the not-so-unpopular conclusion

that these models well might be set aside in favor of a promising new approach. The reason we reached this view is the near exhaustion of the possibilities of introducing the necessary physical parameters that are needed in these models to reveal detailed fission properties. Now that the necessary computational power is available, we have been persuaded that the time has arrived to apply the constrained Hartree-Fock and, eventually, the time-dependent Hartree-Fock method to the fission process.

ACKNOWLEDGMENTS

We are especially pleased to acknowledge Edward Watkins for his assistance in the electronic aspects of our experiments and John Latessa for his superb machine work in constructing our instruments. We also thank the

staff and operating crew of the 88-in. cyclotron at the Lawrence Berkeley Laboratory for their peerless spirit of cooperation and the hundreds of hours of excellent heavy-ion beams. We are indebted for the use of the target materials to the Office of Basic Energy Sciences, U.S. Department of Energy, through the transplutonium production facilities of the Oak Ridge National Laboratory. Two of us (M.S. and K.S.) want to thank the members of the Heavy Element Group for their kind hospitality during our stay at the Lawrence Livermore National Laboratory. Sadly, one of our coauthors, Dr. Glen Bethune, died unexpectedly on May 2, 1988, but we hope he shall be remembered by his fellow scientists. This research was performed under the auspices of the U.S. Department of Energy by the Lawrence Livermore National Laboratory under Contract No. W-7405-Eng-48.

*Present address: Chemistry Department, Brookhaven National Laboratory, Upton, NY 11973.

†Deceased.

¹E. K. Hulet, J. F. Wild, R. J. Dougan, R. W. Loughheed, J. H. Landrum, A. D. Dougan, M. Schädell, R. L. Hahn, P. A. Baisden, C. M. Henderson, R. J. Dupzyk, K. Sümmerer, and G. R. Bethune, *Phys. Rev. Lett.* **56**, 313 (1986).

²For example, M. G. Itkis, V. N. Okolovich, A. Ya. Rusanov, and G. N. Smirenkin, *Z. Phys. A* **320**, 433 (1985); M. G. Itkis, N. A. Kondrat'ev, Yu. V. Kotlov, S. I. Mul'gin, V. N. Okolovich, A. Ya. Rusanov, and G. N. Smirenkin, *Yad. Fiz.* **47**, 7 (1988) [*Sov. J. Nucl. Phys.* **47**, 4 (1988)].

³W. John, E. K. Hulet, R. W. Loughheed, and J. J. Wesolowski, *Phys. Rev. Lett.* **27**, 45 (1971).

⁴D. C. Hoffman, J. B. Wilhelmy, J. Weber, W. R. Daniels, E. K. Hulet, R. W. Loughheed, J. H. Landrum, J. F. Wild, and R. J. Dupzyk, *Phys. Rev. C* **21**, 972 (1980).

⁵E. K. Hulet, R. W. Loughheed, J. H. Landrum, J. F. Wild, D. C. Hoffman, J. Weber, and J. B. Wilhelmy, *Phys. Rev. C* **21**, 966 (1980).

⁶G. Münzenberg, *Rep. Prog. Phys.* **51**, 57 (1988).

⁷J. Randrup, S. E. Larsson, P. Möller, S. G. Nilsson, K. Pomorski, and A. Sobiczewski, *Phys. Rev. C* **13**, 229 (1976).

⁸A. Baran, K. Pomorski, A. Lukasiak, and A. Sobiczewski, *Nucl. Phys. A* **361**, 83 (1981); H. C. Pauli and T. Ledergerber, in *Proceedings of the Symposium on the Physics and Chemistry of Fission, Rochester, New York, 1973* (International Atomic Energy Agency, Vienna, 1974), Vol. I, p. 463.

⁹M. G. Mustafa and R. L. Ferguson, *Phys. Rev. C* **18**, 301 (1978).

¹⁰J. R. Nix, *Annu. Rev. Nucl. Sci.* **22**, 341 (1972).

¹¹U. Mosel, J. Maruhn, and W. Greiner, *Phys. Lett.* **34B**, 587 (1971).

¹²U. Mosel and H. W. Schmitt, *Phys. Rev. C* **4**, 2185 (1971).

¹³M. G. Mustafa, U. Mosel, and H. W. Schmitt, *Phys. Rev. Lett.* **28**, 1536 (1972); M. G. Mustafa, U. Mosel, and H. W. Schmitt, *Phys. Rev. C* **7**, 1519 (1973).

¹⁴J. F. Wild, J. van Aarle, W. Westmeier, R. W. Loughheed, E. K. Hulet, K. J. Moody, R. J. Dougan, R. Brandt, E.-A. Koop, and P. Patzelt, submitted to *Phys. Rev. C*; Lawrence Livermore National Laboratory Report UCAR 10062/88, 1988 (unpublished), p. 132.

¹⁵G. N. Flerov, Yu. Ts. Oganessian, Yu. V. Lobanov, V. I. Kuznetsov, V. A. Druin, V. A. Pereygin, K. A. Gavrilov, S.

P. Tretyakova, and V. M. Poltko, *Phys. Lett.* **12**, 73 (1964).

¹⁶V. A. Druin, Yu. S. Korotkin, Yu. V. Lobanov, Yu. V. Poluboyarinov, R. N. Sagaidak, G. M. Solov'eva, S. P. Tretyakova, and Yu. P. Kharitonov, *Yad. Fiz.* **24**, 254 (1976) [*Sov. J. Nucl. Phys.* **24**, 131 (1976)].

¹⁷V. A. Druin, B. Bochev, Yu. S. Korotkin, V. N. Kosyakov, Yu. V. Lobanov, E. A. Minin, Yu. V. Poluboyarinov, A. G. Rykov, R. N. Sagaidak, S. P. Tretyakova, and Yu. P. Kharitonov, *At. Energ.* **43**, 155 (1977) [*Sov. J. At. En.* **43**, 785 (1977)].

¹⁸J. M. Nitschke, M. Fowler, A. Ghiorso, R. E. Leber, M. E. Leino, M. J. Nurmi, L. P. Somerville, K. E. Williams, E. K. Hulet, J. H. Landrum, R. W. Loughheed, J. F. Wild, C. E. Bemis, Jr., R. J. Silva, and P. Eskola, *Nucl. Phys. A* **352**, 138 (1981).

¹⁹G. M. Ter-Akopian, R. N. Sagaidak, A. A. Pleve, S. P. Tretyakova, G. N. Buklanov, A. G. Artuch, and A. M. Kalinin, Joint Institute for Nuclear Research Report No. P7-634, 1985.

²⁰L. P. Somerville, M. J. Nurmi, J. M. Nitschke, A. Ghiorso, E. K. Hulet, and R. W. Loughheed, *Phys. Rev. C* **31**, 1801 (1985).

²¹E. K. Hulet, in *Proceedings of the International School-Seminar on Heavy-Ion Physics, Alushta, 1983*, Joint Institute for Nuclear Research Report No. D7-83-644, 1983, p. 431.

²²R. W. Loughheed and E. K. Hulet, *Nucl. Instrum. Methods* **166**, 329 (1979).

²³J. M. Nitschke, *Nucl. Instrum. Methods* **138**, 393 (1976).

²⁴R. J. Dougan, P. A. Baisden, and E. K. Hulet (unpublished).

²⁵V. A. Druin, Yu. P. Kharitonov, Yu. S. Korotkin, V. N. Kosyakov, Yu. V. Lobanov, E. A. Minin, Yu. P. Poluboyarinov, A. G. Rykov, R. N. Sagaidak, and S. P. Tretyakova, Joint Institute for Nuclear Research Report No. E7-9546, 1977.

²⁶J. Weber, B. R. Erdal, A. Gavron, and J. B. Wilhelmy, *Phys. Rev. C* **13**, 189 (1976).

²⁷R. Vandenbosch and J. R. Huizenga, *Nuclear Fission* (Academic, New York, 1973), p. 60.

²⁸H. Henschel, A. Kohnle, H. Hipp, and G. Gönnewein, *Nucl. Instrum. Methods* **190**, 125 (1981).

²⁹H. W. Schmitt, W. E. Kiker, and C. W. Williams, *Phys. Rev.* **137**, B837 (1965).

³⁰E. Weissenberger, P. Geltenbort, A. Oed, F. Gönnewein, and H. Faust, *Nucl. Instrum. Methods*, **A248**, 506 (1986).

- ³¹M. Nurmia, K. Eskola, P. Eskola, and A. Ghiorso, Lawrence Berkeley Laboratory Report UCRL-18667, 1969 (unpublished), p. 63.
- ³²R. W. Lougheed, E. K. Hulet, R. L. Landingham, J. M. Nitschke, H. Folger, J. V. Kratz, W. Brüchele and H. Gäggeler, Nucl. Instrum. Methods **200**, 71 (1982).
- ³³E. K. Hulet, J. F. Wild, R. W. Lougheed, J. E. Evans, B. J. Qualheim, M. Nurmia, and A. Ghiorso, Phys. Rev. Lett. **26**, 523 (1971).
- ³⁴E. K. Hulet, R. W. Lougheed, J. F. Wild, R. J. Dougan, K. J. Moody, R. L. Hahn, C. M. Henderson, R. J. Dupzyk, and G. R. Bethune, Phys. Rev. C **34**, 1394 (1986).
- ³⁵R. W. Lougheed, E. K. Hulet, R. J. Dougan, J. F. Wild, R. J. Dupzyk, C. M. Henderson, K. J. Moody, R. L. Hahn, K. Sümmerer, and G. Bethune, J. Less-Common Met. **122**, 461 (1986).
- ³⁶M. Schädel, W. Brüchele, M. Brügger, H. Gäggeler, K. J. Moody, D. Schardt, K. Sümmerer, E. K. Hulet, A. D. Dougan, R. J. Dougan, J. H. Landrum, R. W. Lougheed, J. R. Wild, and G. D. O'Kelley, Phys. Rev. C **33**, 1547 (1986).
- ³⁷J. F. Wild, E. K. Hulet, R. W. Lougheed, P. A. Baisden, J. H. Landrum, R. J. Dougan, and M. G. Mustafa, Phys. Rev. C **26**, 1531 (1982).
- ³⁸R. W. Lougheed *et al.* (unpublished).
- ³⁹R. W. Lougheed, K. J. Moody, R. J. Dougan, J. F. Wild, E. K. Hulet, R. J. Dupzyk, C. M. Henderson, C. M. Gannett, R. A. Henderson, D. C. Hoffman, D. M. Lee, K. Sümmerer, and R. L. Hahn, Lawrence Livermore National Laboratory Report No. UCAR 10062/87, 1987 (unpublished), p. 42.
- ⁴⁰K. J. Moody, R. W. Lougheed, R. J. Dougan, R. W. Hoff, E. K. Hulet, J. F. Wild, R. J. Dupzyk, C. M. Henderson, R. L. Hahn, and G. R. Bethune (unpublished).
- ⁴¹J. R. Alonso, *Gmelin Handbüch der Anorganischen Chemie* (Springer, Berlin, 1974), Vol. 7b, Part A 1, 2, p. 104.
- ⁴²P. F. Dittner, C. E. Bemis, Jr., R. L. Ferguson, F. Plasil, F. Pleasonton, and D. C. Hensley, Phys. Rev. C **23**, 555 (1981).
- ⁴³P. Möller and S. G. Nilsson, Phys. Lett. **31B**, 283 (1970); H. C. Pauli, T. Ledergerber, and M. Brack, *ibid.* **34B**, 264 (1971); G. Gustafsson, P. Möller, and S. G. Nilsson, *ibid.* **34B**, 349 (1971).
- ⁴⁴V. E. Viola, K. Kwiatkowski, and M. Walker, Phys. Rev. C **31**, 1550 (1985).
- ⁴⁵J. P. Unik, J. Gindler, L. Glendenin, K. Flynn, A. Gorski, and R. Sjoblom, *Proceedings of the IAEA Third International Symposium on the Physics and Chemistry of Fission*, Rochester, 1973 (International Atomic Energy Agency, Vienna, 1974), Vol. II, p. 51.
- ⁴⁶U. Brosa, S. Grossmann, and A. Müller, Z. Phys. A **325**, 242 (1986); V. V. Pashkevich and A. Sandulescu, Joint Institute for Nuclear Research Report No. 16-86, 1986, pp. 19–23; K. Depta, J. A. Maruhn, W. Greiner, W. Scheid, and A. Sandulescu, Mod. Phys. Lett. A **1**, 377 (1986); V. V. Pashkevich, Nucl. Phys. **A477**, 1 (1988); S. Cwiok, P. Rozmej, and A. Sobiczewski, in *Nuclei Far from Stability*, Proceedings of the 5th International Conference on Nuclei Far from Stability, AIP Conf. Proc. No. 164, edited by I. S. Towner (AIP, New York, 1988), p. 821; S. Cwiok, P. Rozmej, A. Sobiczewski, and Z. Patyk, Nucl. Phys. **A491**, 281 (1989).
- ⁴⁷P. Möller, J. R. Nix, and W. J. Swiatecki, Nucl. Phys. **A469**, 1 (1987); **A492**, 349 (1989).
- ⁴⁸A. Turkevich and J. B. Niday, Phys. Rev. **84**, 52 (1951).
- ⁴⁹H. B. Levy, H. G. Hicks, W. E. Nervik, P. C. Stevenson, J. B. Niday, and J. C. Armstrong, Jr., Phys. Rev. **124**, 544 (1961).
- ⁵⁰R. C. Ragaini, E. K. Hulet, R. W. Lougheed, and J. F. Wild, Phys. Rev. C **9**, 399 (1974).
- ⁵¹H. C. Britt, D. C. Hoffman, J. van der Plicht, J. B. Wilhelmy, E. Cheifetz, R. J. Dupzyk, and R. W. Lougheed, Phys. Rev. C **30**, 559 (1984).
- ⁵²R. W. Lougheed, E. K. Hulet, J. F. Wild, K. J. Moody, R. J. Dougan, C. M. Gannett, R. A. Henderson, D. C. Hoffman, and D. M. Lee, Lawrence Livermore National Laboratory Report No. UCAR 10062/88, 1988 (unpublished), p. 135.
- ⁵³C. E. Bemis, Jr., R. L. Ferguson, F. Plasil, R. J. Silva, G. D. O'Kelley, M. L. Kiefer, R. L. Hahn, C. C. Hensley, E. K. Hulet, and R. W. Lougheed, Phys. Rev. Lett. **39**, 1246 (1977).
- ⁵⁴V. V. Pashkevich, Nucl. Phys. **A169**, 275 (1971); M. G. Mustafa, U. Mosel, and H. W. Schmitt, Phys. Rev. C **7**, 1519 (1973).